Enhancement of Optical Anisotropy by Interconnection Effect along Growth Direction in Multistacked Quantum Dots

Tanaka, Hideharu
Kojima, Osamu
Kita, Takashi
Akahane, Kouichi

(Citation)
Japanese Journal of Applied Physics,52:012001-012001

(Issue Date)
2013

(Resource Type)
journal article

(Version)
Accepted Manuscript

Enhancement of Optical Anisotropy by Interconnection Effect along Growth Direction in Multistacked Quantum Dots

Hideharu Tanaka[1], Osamu Kojima[1]*, Takashi Kita[1], and Kouichi Akahane[2]

[1]*Department of Electrical and Electronic Engineering, Graduate School of Engineering, Kobe University, Kobe 657-8501, Japan*

[2]*National Institute of Information and Communications Technology, Koganei, Tokyo 184-8795, Japan*

We report the enhancement of in-plane optical anisotropy in stacked InAs quantum dots (QDs) with a decrease in spacer layer thickness. The in-plane polarization anisotropy of photoluminescence intensity is basically due to the ellipsoidal QD shape caused by lattice mismatch strain. The polarization degree increases to approximately 40% with decreasing spacer layer thickness. When the spacer layer thickness decreases, the electron envelope function becomes longer along the growth direction, which is the interconnection effect. This interconnection results in the enhancement of the in-plane anisotropy. These results exhibit that the vertical interaction by the interconnection effect is an important factor for the QD optical anisotropy.

1. Introduction

Semiconductor quantum dots (QDs) are a promising zero-dimensional quantum structure for applications in various optical devices.[1–5] When the self-assembled QDs are fabricated from two-dimensional to three-dimensional island growth using the Stranski-Krastanov growth-mode transition, they are elliptical because of the dependence of the diffusion length of the atoms in the in-plane direction.[6] In addition to this elliptical shape, the anisotropic strain causes the anisotropic electronic state. Since the optical characteristics strongly depend on the electronic state, the modified electronic states result in optical anisotropy. Many reports have discussed the QD optical anisotropy in the in-plane direction, which mainly arises from heavy-hole (HH) -light-hole mixing in the valence band Luttinger Hamiltonian.[7–10]

We have demonstrated the optical characteristics of the stacked InAs QDs grown on an InP (311)B substrate using a strain-compensation technique to fabricate high-density QD ensembles without dislocations[11–13] as the control method for the exciton characteristics.[14–18] As we have reported, a decrease in the growth-direction QD separation

*E-mail address: kojima@phoenix.kobe-u.ac.jp

induces the change in the quantum confinement effects. While the HH forming excitons are strongly localized in QD, the electron envelope functions tunnel to the spacer layers (i.e., barrier layers) because of the difference in the less effective mass. When the spacer layer thickness d decreases, the electrons approach each other along the growth direction and the electron envelope functions overlap within the spacer layer, which is called the interconnection effect of electron envelope functions along the growth direction. Since this interconnection effect leads to the reduction in the magnitude of the overlap integral between the electron and hole envelope functions, the exciton oscillator strength reduces with decreasing the spacer layer thickness; this causes the decrease in the photoluminescence (PL) intensity and the increase in the PL decay time. Moreover, this interconnection effect causes the PL energy shift to the lower energy side by the expansion of the confinement volume owing to the interconnection of electron envelope functions. This expansion was directly shown by the enhancement of the transverse-magnetic mode of the cleaved edge emission. Here, the key point of the interconnection in our previous reports is that only the electron expands along the growth direction. Therefore, unless holes interact with each other, the interconnection strength increases with the decrease in d, which means a further decrease in the oscillator strength.

On the other hand, in the InAs QDs grown on InP (311)B substrates, the PL intensity in the $[\bar{2}33]$ polarization direction is greater than that in the $[01\bar{1}]$ polarization direction[19,20] because of the anisotropy of the exciton dipole moment.[21] When the interconnection effect induced by the reduction in d causes the change in the electronic state, this value of the anisotropy should depend on d. In the present study, we systematically investigate the relationship between d and the PL anisotropy in stacked InAs self-assembled QDs. The in-plane polarization degree clearly depends on d. We discuss the d dependence of the anisotropy from the viewpoint of lengthening of the electron envelope function along the growth direction.

2. Experimental Procedure

We used four samples in the present work. Each sample consisting of InAs self-assembled QD layers with 30 periods was grown on an InP (311)B substrate by solid-source molecular beam epitaxy using the strain compensation technique.[15] The InGaAlAs spacer layer compensates for the stress caused by the lattice mismatch with a QD layer, and the thickness d was changed from 10 to 40 nm. In the case of $d = 20$, 30, and 40 nm, the composition of the spacer layer is $In_{0.5}Ga_{0.1}Al_{0.4}As$, and in the case of $d = 10$ nm, it is

$In_{0.47}Ga_{0.10}Al_{0.43}As$ because of the stress difference. Hereafter, we denote each sample as "$d = x$ nm sample" ($x = 10$, 20, 30, and 40). In our previous report,[15] while there is no interaction between the QD layers along the growth direction in the $d = 40$ nm sample, the QDs in the $d < 40$ nm samples are partially or strongly interconnected along the growth direction via the electron envelope function. The interconnection increases the exciton lifetime due to a decrease in oscillator strength. The QD PL polarization was characterized by measuring the conventional PL spectrum. The excitation source was a mode-locked Ti:sapphire laser used as a continuous-wave mode. The excitation energy was tuned to 1.38 eV to eliminate the contribution of the carriers excited in the spacer layers. The emitted light was dispersed by a 32 cm single monochromator with a resolution of 6.0 nm and detected by a liquid-nitrogen-cooled InGaAs-photodiode array. The excitation density was 0.75 W/cm^2, and the polarization of the excitation beam was parallel to the $[01\bar{1}]$ polarization direction. All measurements were performed at 5 K.

3. Results and Discussion

At first, we show the analysis results of the QD shape measured by atomic force microscopy (AFM). Figure 1(a) indicates the relationship between the QD lengths of the $[01\bar{1}]$ $L_{[01\bar{1}]}$ and $[\bar{2}33]$ $L_{[\bar{2}33]}$ directions in all samples. The size of 20 QDs was measured in each sample. The dotted line indicates that the ratio of the lengths is unity; the QDs on this line have the round shape. Figure 1(b) depicts the average ratio of the lengths. If the oval shape is a main reason for the optical anisotropy, the $d = 20$ and 30 nm samples will hardly show the anisotropy because the length ratios are approximately unity.

There is no reference that explains this dependence; therefore, we considered that the difference in the interaction of the strain fields induced by the lattice mismatch due to changing d causes this dependence of the shape. It is well known that the surface after the growth of the spacer layer becomes almost flat, and that the QDs on the spacer layer are formed on the QDs underneath the spacer layer owing to the strain fields.[22,23] From this aspect, the strain fields strongly affect the QD formation at $d = 10$ nm, so that the shape is similar underneath the structure. Therefore, the QDs have an elliptical shape. Furthermore, in the case of the $d = 20$ and 30 nm, the strain fields are averaged by the nearest neighbor fields, which leads to a round shape. Moreover, as d increases, the spacer layer perfectly averages the strain fields; the QD formation

condition is reset, so that the QDs show an elliptical shape as same as the first layer. This dependence of the averaging of the strain field on d is attributed to the QD shape variation.

The solid and dashed curves in Fig. 2 show the PL spectra of each sample measured in the $[\bar{2}33]$ and $[01\bar{1}]$ polarization directions, respectively. The dip at approximately 0.9 eV is because of absorption by the hydroxyl group in the optical fiber. The change in the PL spectra with varying d originates from the interconnection effect of QDs.[15] In all samples, the PL intensity along the $[\bar{2}33]$ polarization direction is greater than that along the $[01\bar{1}]$ polarization direction. Moreover, the ratio of the PL peak intensity along the $[\bar{2}33]$ polarization direction to that along the $[01\bar{1}]$ polarization direction clearly increases with decreasing d. For example, this ratio is 1.42 for the $d = 40$ nm sample, whereas it is 2.42 for the $d = 10$ nm sample. This result cannot be explained by the analysis result of the QD shape as shown in Fig. 1.

To clarify the polarization properties for each sample, the dependence of the PL spectrum on the detection angle was measured. Figure 3(a) shows a summary of the results. The degree of polarization P is defined as follows:

$$P = \frac{I_{[\bar{2}33]} - I_\theta}{I_{[\bar{2}33]} + I_\theta}, \tag{1}$$

where $I_{[\bar{2}33]}$ is the PL peak intensity in the $[\bar{2}33]$ polarization direction and I_θ is that at an angle of θ from the $\langle 01\bar{1}\rangle$ axis, as shown in the inset of Fig. 3(a). The dashed lines at 0°, 90°, and 180° represent the $[01\bar{1}]$, $[\bar{2}33]$, and $[01\bar{1}]$ polarization directions, respectively. In all samples, P reaches a maximum in the $[01\bar{1}]$ polarization direction and shows a minimum in the $[\bar{2}33]$ polarization direction.

When there is no interaction between QDs along the growth direction, the in-plane optical anisotropy in QDs mainly originates from the difference in the strain effect along the $[\bar{2}33]$ and $[01\bar{1}]$ directions induced by the elliptical shape of the QDs. In the case of the multilayered InAs QD ensembles with $d = 60$ nm grown on an InP (311)B substrate, the $[\bar{2}33]$ polarization direction of the PL intensity is largest[19,21] owing to the light-hole-like ground state preferentially polarized along the $[\bar{2}33]$ direction.[7]

For the $d = 40$ nm sample without the interconnection effect, the polarization degree $P = 14\%$, which is close to the reported value of 16 - 19% in the sample with $d = 60$ nm.[19,20] Thus, we concluded that the polarization in strain-compensated InAs QDs on an InP (311)B substrate without the interconnection effect is approximately 15%. On the other hand, with decreasing d, P increases up to 41% in the $d = 10$ nm

sample. Since the excitation energy of 1.38 eV is less than the band gap energy of the $In_{0.47}Ga_{0.10}Al_{0.43}As$-spacer layer,[18] the enhancement of the polarization is attributed to the changes in the optical characteristics of the QDs induced by the interconnection effect on the electron states.

The polarization degree along the $[01\bar{1}]$ direction is plotted as a function of the inverse of d in Fig. 3(b). The dotted curve indicates the dependence of the polarization degree on $1/d$. In the simple model of the quantum well with the finite potential barrier, it is well known that the amplitude of the envelope function in the well decreases in the barrier layers by a function of $\exp(-\gamma x)$, where γ is the damping factor and x is the position coordinate. Hence, the interconnection strength is proportional to $1/d$. This plot shows that the increase in the polarization degree is caused by a one-dimensional change in the confinement volume; the decrease in d induces the overlap of the electron envelope function along the growth direction in the spacer layers, and the increase in the overlap enhances the polarization degree. The interconnection effect makes the confinement along the growth direction weak, while the in-plane confinement decides the basic characteristics. The change in the confinement effect due to the elongation of the envelope function along the growth direction varies with the in-plane confinement, which induces the change in anisotropic PL.

To compare the increase in optical anisotropy due to the interconnection effect with that due to the increase in QD height, we focused on the PL-energy dependence of the polarized PL. Figure 4 shows the average QD height in the samples determined from analysis of the AFM images obtained. The average QD height is almost constant, approximately 6 nm. This indicates that the variation of QD height is not the main reason for the enhancement of the polarization degree.

Figure 5 shows the dependence of the PL intensity ratio in the $[\bar{2}33]$ polarization direction to that in the $[01\bar{1}]$ polarization direction as a function of PL energy in all samples. In the $d = 30$ and 40 nm samples, the PL energy dependence is small and almost the same. The decrease in PL energy, namely, the decrease in the band gap energy of QDs, is caused by the increase in QD height in the ensembles.[?,?,24,25] Therefore, although the slight increase in QD height increases the anisotropy, the dependence is very small.

On the other hand, in the samples $d = 20$ and 10 nm, the PL intensity ratios exhibit peaks at energies different from the PL peak energies indicated by arrows. In the higher-energy region, the PL ratio increases with decreasing PL energy. Although

the averaged QD height is almost 6 nm, as shown in Fig. 4, the QD ensemble has the size distribution corresponding to the PL width, which is mainly height distribution. Therefore, the increase in QD height induces the strengthening of interconnections, so that the anisotropy increases with decreasing the PL energy.

In the lower-energy region, the PL ratio decreases with decreasing the PL energy. The theoretical reason for this decrease is unclear, so that we speculated as follows; the QD separations in the lower PL energy region are closer than that in the higher PL energy region. In the case of the moderate separation, the interconnection via the electron envelope function changes the exciton characteristics and enhances the optical anisotropy. However, in the case of the closer QD separation, the interconnection via the hole envelope function will be induced. This hole interconnection may decrease the anisotropy, because the spatial carrier separation decreases. The electron interconnection induces the spatial separation of electrons and holes, which leads to the decrease in the oscillator strength. On the other hand, the hole interconnection cancels the spatial separation effects. Therefore, the increase in the QD height induced by the electron and hole interconnection effects results in the peak structure. The balance between the change in the interconnection and quantum confinement may be attributed to the flat region in the result of $d = 10$ nm shown in Fig. 5.

4. Conclusions

We found that the optical anisotropy clearly inversely depends on the spacer thickness in stacked QDs fabricated using the strain compensation technique and that there is a possibility that the interconnection effects enhance the in-plane anisotropy. To clarify the origin of this enhancement, we examined the PL-energy dependence of the ratio of the PL intensity in the $[\bar{2}33]$ and $[01\bar{1}]$ polarization directions. The results imply that the electron envelope function becoming longer along the growth direction increases the optical anisotropy. These results are an important to consider in designing QD optical devices, in particular, vertical structure devices including vertical cavity surface emitting lasers and solar cells.

Acknowledgment

This work was partially supported by a Grant-in-Aid for Scientific Research (No. 23656050) from the Ministry of Education, Culture, Sports, Science, and Technology of Japan, the Incorporated Administrative Agency NEDO of Japan.

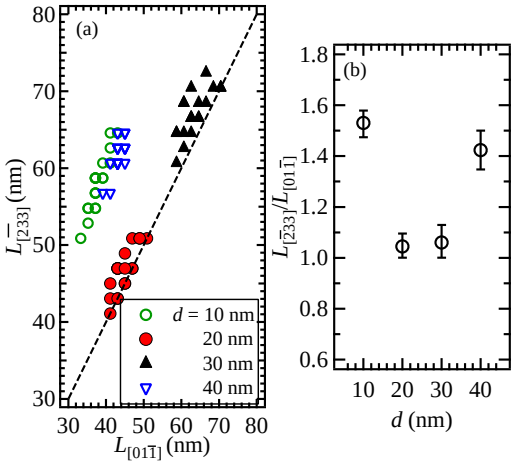

Fig. 1. (Color online) (a)Analysis results for the QD shape in the samples. The dotted line indicates that the ratio of $L_{[01\bar{1}]}$ to $L_{[\bar{2}33]}$ is unity. (b)The average ratio of $L_{[01\bar{1}]}$ to $L_{[\bar{2}33]}$ is plotted as a function of d.

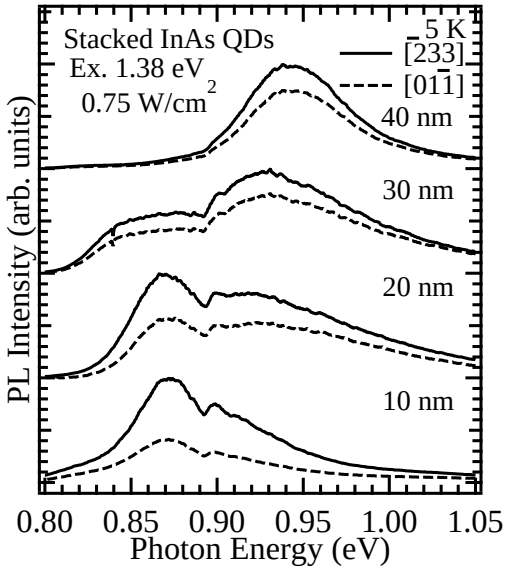

Fig. 2. PL spectra of the stacked QDs with various d values at 3.5 K. The solid and dashed curves indicate the PL spectra in the [$\bar{2}$33] and [01$\bar{1}$] polarization directions, respectively.

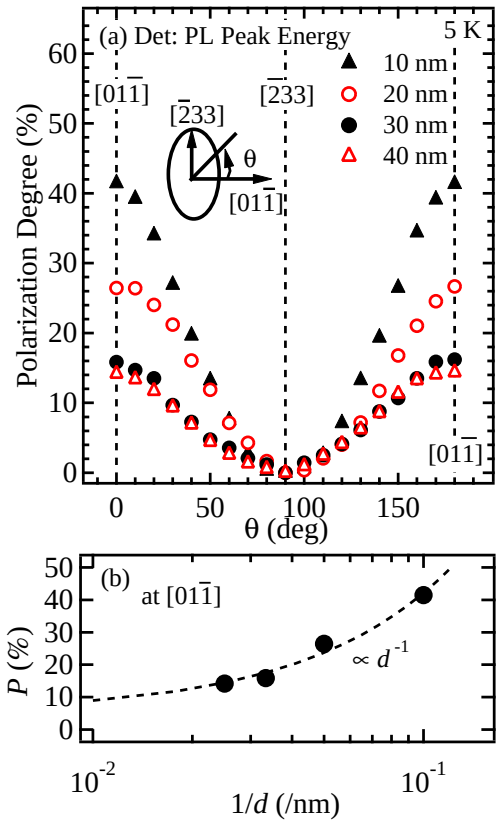

Fig. 3. (Color online) (a)Dependence of degree of polarization on detection angle for samples of varying thicknesses. The dashed lines at 0 and 180° indicate the $[01\bar{1}]$ polarization direction, and that at 90° indicates the $[\bar{2}33]$ polarization direction. Inset shows the geometry defining the angle (θ). (b)P in the $[01\bar{1}]$ polarization direction plotted as a function of $1/d$. The dashed curve shows the fitting one.

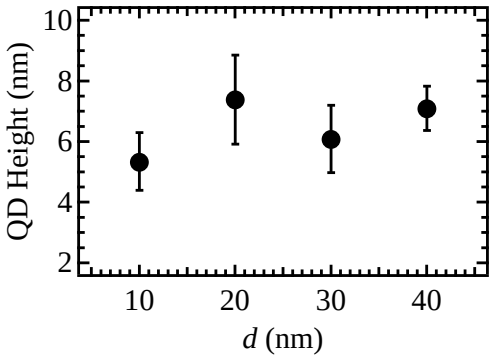

Fig. 4. Analysis result for the QD height in each sample.

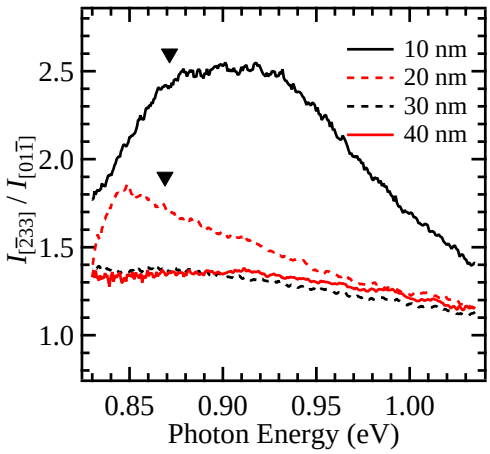

Fig. 5. (Color online) Ratio of PL intensity in $[\bar{2}33]$ polarization direction to that in $[01\bar{1}]$ polarization direction as a function of PL energy for the samples of various d values. The arrows indicate the PL peak energies in the $d = 10$ and 20 nm samples.

References

1) D. L. Huffaker, G. Park, Z. Zou, O. B. Shchekin, and D. G. Deppe: Appl. Phys. Lett. **73** (1998) 2564.
2) R. Prasanth, J. E. M. Haverkort, A. Deepthy, E. W. Bogaart, J. J. G. M. van der Tol, E. A. Patent, G. Zhao, Q. Gong, P. J. van Veldhoven, R. Nötzel, and J. H. Wolter: Appl. Phys. Lett. **84** (2004) 4059.
3) E. W. Bogaart, R. Nötzel, Q. Gong, J. E. M. Haverkort, and J. H. Wolter: Appl. Phys. Lett. **86** (2005) 173109.
4) A. Martí, E. Antolín, C. R. Stanley, C. D. Farmer, N. López, P. Díaz, E. Cánovas, P. G. Linares, and A. Luque: Phys. Rev. Lett. **97** (2006) 247701.
5) R. Oshima, A. Takata, and Y. Okada: Appl. Phys. Lett. **93** (2008) 083111.
6) T. Inoue, T. Kita, O. Wada, M. Konno, T. Yaguchi, and T. Kamino: Appl. Phys. Lett. **92** (2008) 031902.
7) M. Henini, S. Sanguinetti, S. C. Fortina, E. Geilli, M. Guzzi, G. Panzarini, L. C. Andreani, M. D. Upward, P. Moriarty, P. H. Beton, and L. Eaves: Phys. Rev. B **57** (1998) 6815.
8) L. W. Wang, J. Kim, and A. Zunger: Phys. Rev. B **59** (1999) 5678.
9) S. Sanguinetti, S. Castiglioni, E. Grilli, M. Guzzi, G. Panzarini, L. C. Andreani, and M. Henini: Jpn. J. Appl. Phys. **38** (1999) 4676.
10) S. Cortez, O. Krebs, P. Voisin, and J. M. Gérard: Phys. Rev. B **63** (2001) 233306.
11) K. Akahane, N. Ohtani, Y. Okada, and M. Kawabe: J. Cryst. Growth **245** (2002) 31.
12) K. Akahane, N. Yamamoto, and M. Tsuchiya: Appl. Phys. Lett. **93** (2008) 041121.
13) K. Akahane, N. Yamamoto, and T. Kawanishi: Phys. Status Solidi A **208** (2011) 425.
14) H. Nakatani, T. Kita, O. Kojima, O. Wada, K. Akahane, and M. Tsuchiya: J. Lumin. **128** (2008) 975.
15) O. Kojima, H. Nakatani, T. Kita, O. Wada, K. Akahane, and M. Tsuchiya: J. Appl. Phys. **103** (2008) 113504.
16) O. Kojima, H. Nakatani, T. Kita, O. Wada, and K. Akahane: J. Appl. Phys. **107** (2010) 073506.
17) O. Kojima, M. Mamizuka, T. Kita, O. Wada, and K. Akahane: Phys. Status Solidi C **8** (2011) 46.

18) O. Kojima, N. Tobita, T. Kita, and K. Akahane: J. Appl. Phys. **110** (2011) 093515.

19) M. Kujiraoka, J. Ishi-Hayase, K. Akahane, N. Yamamoto, K. Ema, and M. Sasaki: AIP Conf. Proc. **893**, PHYSICS OF SEMICONDUCTORS: 28th Int. Conf. on the Physics of Semiconductors - ICPS 2006, 2007, p.975.

20) M. Kujiraoka, J. Ishi-Hayase, K. Akahane, N. Yamamoto, K. Ema, and M. Sasaki: J. Lumin. **128** (2008) 972.

21) J. Ishi-Hayase, K. Akahane, N. Yamamoto, M. Sasaki, M. Kujiraoka, and K. Ema: Appl. Phys. Lett. **91** (2007) 103111.

22) Y. Nakayama, O. G. Schmidt, N. Y. Jin-Phillipp, S. Kiravittaya, C. Müller, K. Eberl, H. Gräbeldinger, and H. Schweizer: J. Cryst. Growth **242** (2002) 339.

23) P. M. Lytvyn, Y. I. Mazur, E. Marega Jr., V. G. Dorogan, V. P. Kladko, M. V. Slobodian, V. V. Strelchuk, M. L. Hussein, M. E. Ware, and G. J. Salamo: Nanotechnology **19** (2008) 505605.

24) C. Cornet, A. Schliwa, J. Even, F. Dor´e, C. Celebi, A. L´etoublon, E. Mac´e, C. Parantho¨en, A. Simon, P. M. Koenraad, N. Bertru, D. Bimberg, and S. Loualiche: Phys. Rev. B 74 (2006) 035312.

25) Y. I. Mazur, S. Noda, G. G. Tarasov, V. G. Dorogan, G. J. Salamo, O. Bierwagen, W. T. Masselink, E. A. Decuir, Jr., and M. O. Manasreh: J. Appl. Phys. 103(2008) 054315.